

# 1 Soil carbon accrual and biopore formation across a plant 2 diversity gradient

3 Kyungmin Kim<sup>1,2,3,4</sup>, Maik Geers-Lucas<sup>5</sup>, G. Philip Robertson<sup>3,4,6</sup> and Alexandra  
4 Kravchenko<sup>3,4</sup>

5 <sup>1</sup>Department of Agricultural Biotechnology, Seoul National University, Seoul, Korea

6 <sup>2</sup>Institute of Plant Environmental Science, Research Institute of Agriculture and Life Sciences, Seoul National  
7 University, Seoul, Korea

8 <sup>3</sup>Department of Plant Soil and Microbial Sciences, Michigan State University, East Lansing, MI, USA

9 <sup>4</sup>DOE Great Lakes Bioenergy Research Center, Michigan State University, East Lansing, MI, USA

10 <sup>5</sup>Department of Soil Science, Technische Universität Berlin, Germany

11 <sup>6</sup>W.K. Kellogg Biological Station, Michigan State University, Hickory Corners, MI, USA

12 Correspondence to: Kyungmin Kim (km\_kim@snu.ac.kr)

13 **Abstract.** Plant diversity promotes soil organic carbon (SOC) gains through intricate changes in root-soil  
14 interactions and their subsequent influence on soil physical and biological processes. We assessed SOC and pore  
15 characteristics of soils under a range of switchgrass-based plant systems, representing 12 years after their  
16 establishment. The systems represented a gradient of plant diversity with species richness ranging from 1 to 30  
17 species 12 years after their establishment. We focused on soil biopores as indicators of the legacy of root activity  
18 legacy, measured using X-ray computed micro-tomography scanning, and explored biopore relationships with  
19 SOC accumulation. Biopores were measured using X-ray computed micro-tomography.

20 Plant functional richness explained 29% of bioporosity and 36% of SOC variation, while bioporosity itself  
21 explained 36% of the variation in SOC. The most diverse plant system (30 species) had the highest SOC, while  
22 long-term bare soil fallow and monoculture switchgrass had the lowest. Of particular note was a two-species  
23 mixture of switchgrass (*Panicum virgatum* L.) and ryegrass (*Elymus canadensis*), which exhibited the highest  
24 bioporosity and achieved SOC levels comparable to those of the systems with 6 and 10 plant species, and were  
25 inferior only to the system with 30 species. We conclude that plant diversity may enhance SOC through biopore-  
26 mediated mechanisms and suggest a potential for identifying specific plant combinations that may be particularly  
27 efficient for fostering biopore formation and, subsequently, SOC sequestration.

28

## 29 **1 Introduction**

30 Plant diversity has been found to positively influence soil organic carbon (SOC) accumulation in various  
31 ecosystems, including grasslands (Lange et al., 2015; Sprunger and Robertson, 2018) and row crop agriculture  
32 (Liebman et al., 2013; McDaniel et al., 2014). Among the mechanisms through which higher plant diversity  
33 promotes SOC storage are i) high biomass and C inputs from roots (Yang and Tilman, 2020), ii) slower root  
34 decomposition in high diversity systems due to increased root C:N ratios (Chen et al., 2017), and iii) higher  
35 microbial activity enhanced by belowground inputs, where greater quantities of plant-added C are being  
36 microbially processed and transformed into microbial biomass (Prommer et al., 2020; Lee et al., 2023) and then  
37 necromass (Qian et al., 2023; Mou et al., 2024). This microbially-processed C is then protected through physico-  
38 chemical associations with soil minerals (Cotrufo et al., 2022). Moreover, in diverse plant communities

서식 지정함: 글꼴: 기울임꼴

서식 지정함: 글꼴: 기울임꼴

서식 지정함: 글꼴 색: 자동

39 The quantity and chemical composition of C inputs from plant roots and soil biota play an important role in ensuring SOC gains (Berhongaray et al., 2019; Lehmann et al., 2020). For instance, extensive root growth and earthworm activity can facilitate the root exudates and earthworm secretions, which in turn stimulate microbial growth, C assimilation (Kuzyakov and Blagodatskaya, 2015), and the accumulation of microbial necromass (Banfield et al., 2018). Yet, the specific locations within the soil matrix where such inputs are added and their spatial distribution patterns can be an important driver in formation of SOC and its subsequent protection. In diverse plant communities, belowground competition among plants with contrasting root architectures can lead to greater root proliferation through the soil matrix, thereby increasing the density and spatial distribution of root channels that are in direct contact with the soil matrix (Gersani et al., 2001; Bargaz et al., 2017; Wang et al., 2017). More extensive and dense root growth results in greater volumes of the soil matrix being exposed to inputs. Similarly, diverse plant communities exhibit increased activity of soil mesofauna such as earthworms, whereby earthworms create new root-derived biogenic channels that expand the contact surface between soil and organic material and subsequent microbial activities (Kravchenko et al., 2019). However, spatial distributions (Milcu et al., 2019) of these soil-organic matter interfaces varies considerably with plant diversity and species composition (Marshall et al., 2016; Zahorec et al., 2022). For instance, shifts in root morphology and spatial distribution in response to neighboring plant species can vary (Bolte and Villanueva, 2006; Wang et al., 2014), thereby producing root-soil interactions unique to indicate that the formation of root-derived channels and the localization of C storage depend on community composition. Likewise, findings that earthworm activity differs according to specific plant communities. Moreover, recent evidence has shown that root-soil interactions and plant-derived C gains can also be affected by soil pore structure (Quigley and Kravchenko, 2022; Lueas et al., 2023). The presence of legumes (Eisenhauer et al., 2009) suggest that both the quantity and spatial pattern of SOC storage depend on plant species identity and diversity.

62 Analysis of root-soil and mesofauna-soil interactions in diverse perennial plant communities in situ is extremely challenging due to the opaque nature of soil and the difficulty of carrying out long-term (e.g., multiyear) continuous rhizobox or greenhouse studies. Thus, much knowledge regarding impacts of diverse communities on root-soil interactions is based on speculations from the data on root volumes and architecture generated upon disturbing the system to procure the roots and upon conducting the root measurements after cleaning away the soil (Lange et al., 2015). Likewise, earthworm-soil interactions have often been examined by simple comparisons between earthworm activity and soil carbon, while only a few studies have employed the technically demanding approach of artificially creating earthworm biopores with spatial information (Hoang et al., 2016). In contrast, sampling intact soil from long-term field studies and visualizing root residues, particulate organic matter (POM), and pores via X-ray computed micro-tomography ( $\mu$ CT) can generate helpful information on root-soil interactions, augmenting data from destructive root system analyses (Helliwell et al., 2013), and earthworm-soil interactions (Helliwell et al., 2013). This is where identification and quantification of biopores can be particularly advantageous, because it allows capturing the legacy of root and mesofauna proliferation through the soil matrix and estimating the volume of the soil matrix that has received their C inputs in the past.

76 We surmise that information on biopores from  $\mu$ CT scanning can be of particular relevance for assessing 77 root impacts and root-soil interactions in perennial plant systems. Biopores are the soil pores originated from 78 biological activity such as plant root growth and the movement of earthworms and other soil fauna (Dexter, 1986;

79 Blackwell et al., 1990). Root-originated biopores act as preferential pathways for root growth, organic matter  
80 inputs, water, and nutrient flow, thereby creating microenvironments that favor microbial colonization and  
81 necromass accumulation (Guhra et al., 2022; Kautz et al., 2015; Wendel et al., 2022). Root-originated biopores,  
82 formed either by growth of living roots or by decomposition of old roots, are particularly significant as they are  
83 40 times more abundant, especially in subsoils, compared to earthworm biopores (Banfield et al., 2018). Root  
84 biopores are tubular, round-shaped channels with sizes ranging from a few micron to several centimeters (Kautz,  
85 2015). Since root inputs are primarily introduced into the soil through the biopores, they have >2.5 times higher  
86 soil C contents compared to bulk soil (Banfield et al., 2017). Rapid microbial decomposition of plant residues and  
87 accumulation of microbial residues observed in root biopores (Banfield et al., 2018) suggest that root biopore  
88 characteristics may reflect the physical preferences and biochemical processes involved in the transformation and  
89 accumulation of plant-derived C.

90 Reuse of existing biopores by newly grown roots is a commonly observed process in annual crops such  
91 as wheat, fodder radish, and spring barley (White and Kirkegaard, 2010; Wahlström et al., 2021). Switchgrass, a  
92 North American prairie grass, currently actively explored as a potential bioenergy feedstock (Larnaudie et al.,  
93 2022; Zegada-Lizarazu et al., 2022), is known for its particularly active use of old root channels (i.e., biopore  
94 reuse), especially when grown in monoculture (Lucas et al., 2023). Because of their continuous reuse,  
95 accompanied by repeated influxes of new C and stimulated microbiota, biopores in perennial plant systems can  
96 be viewed as hotspots of C processing and are both a product of historic root-soil interactions and a current arena  
97 of such interactions. Taken together, these considerations suggest that the morphology and spatial pattern of root  
98 biopores may serve as an informative indicator of root-derived SOC within the soil matrix. X-ray µCT is  
99 particularly suitable for biopore investigation (Wendel et al., 2022), enabling the examination of accumulated  
100 evidence of past root-soil interactions.

101 We posit that biopore information derived from X-ray µCT is particularly informative for assessing root  
102 impacts and root-soil interactions in perennial plant systems. In species-rich perennial communities, interspecific  
103 interactions generate complex root architectures and heterogeneous rooting pathways, which in turn produce  
104 spatially variable inputs of root-derived SOC (Zahorec et al., 2021). In this context, increased root-originated  
105 biopores (e.g., the volume fraction and connectivity) can indicate diversified root growth paths and intensified  
106 root-soil contact in perennial systems. Accordingly, we hypothesize that in systems with varying levels of higher  
107 plant diversity promotes the abundance and formation of root biopores and that this enhanced biopore formation  
108 and their development is associated with greater abundance can stimulate C gains. Here we examine SOC. Specifically,  
109 our objectives are to examine first, (i) how a plant diversity gradient comprised of 1 to 30 North America prairie  
110 species can shape soil-pore characteristics, especially with emphasis on biopores, and second, (ii)  
111 whether these characteristics are the (bio)pore abundance is associated with SOC levels accumulated over  
112 the preceding 12 years.

113 **2 Materials and Methods**

114 **2.1 Experimental site and soil sampling**

115 Soil samples were collected from the Cellulosic Biofuel Diversity Experiment site established in 2008  
116 at Kellogg Biological Station (KBS, 42°23'47" N, 85°22'26" W), a part of the KBS Long-Term Ecological  
117 Research (LTER) program (Robertson and Hamilton, 2015). The soil is fine-loamy, mixed, mesic, Typic  
118 Hapludalf (Kalamazoo loam). The experiment consists of twelve plant systems representing a 12-point gradient  
119 of plant diversity, (CE1-CE12), six of which were used in this study. Specifically, we sampled a bare soil system,  
120 which was kept free of vegetation since 2016 after 8 years of continuous corn (CE1), a monoculture switchgrass  
121 (*Panicum virgatum*, L.; var. Southlow) system (CE7), a mixture of two grass species, namely, switchgrass and  
122 Canadian rye (*Elymus canadensis*, L.) (CE8), a mixture of six native grasses (CE9), a mixture of six native grasses  
123 and four forbs (CE10), and a mixture of six native grasses and 24 forbs (CE12). Plant species of each system are  
124 listed in Supplementary Table S1. The experiment is in a randomized complete block design with four replicated  
125 9.1 m x 27.4 m plots for each plant system. (<https://lter.kbs.msu.edu/research/long-term-experiments/cellulosic-biofuels-experiment/>).

126 ~~Aboveground biomass of the plots, except for CE1 (bare soil), was sampled every fall from 2010–2019 (Fig. S1a), and the data of 2018 and 2019 was used for this study (Fig. S1b). The entire aboveground biomass from each plot was harvested with a mini combine, leaving 10–15 cm of stubble, and weighed and subsampled for moisture content determination.~~

127 For soil pore analysis, intact soil cores (5 cm diameter (Ø) and 5 cm height) were taken from the 7–12 cm depth interval in July 2019. ~~This depth encompasses the zone of greatest fine-root abundance and turnover, where root-derived C inputs and microbial activity are most pronounced (Halli et al., 2022; Roosendaal et al., 2016).~~ Loose soil adjacent to each core was also procured for measurements of other soil characteristics. Two soil cores were collected from each plot, for a total of 48 soil cores (6 systems x 4 replicate plots x 2 cores per plot).  
128 ~~Aboveground biomass was measured each autumn (Oct–Nov) from 2010 to 2019 in all plots except CE1 (bare soil) (Fig. S1a). For the present analysis, we used the 2018 and 2019 biomass datasets (Fig. S1b). Soil sampling for this study occurred in July 2019; thus, the 2019 fall biomass provides the most temporally proximate estimate of aboveground production for the soils analyzed, while the 2018 biomass offers the preceding-year context and helps mitigate interannual variability. The entire aboveground biomass from each plot was harvested with a mini combine, leaving 10–15 cm of stubble, and weighed and subsampled for moisture content determination.~~

143 **2.2 Soil characteristics measured using destructively sampled soil**

144 Soil moisture at the time of core sampling was determined gravimetrically using a 20 g subsample of loose soil immediately upon collection. The remaining loose soil samples were air-dried for 2 days and sieved to  
145 < 2 mm for further analysis.

146 ~~Total SOC and total C and N were measured by combustion analysis using an elemental CN analyzer (Costech Analytical Technologies Inc., CA, USA). Soil CSOC mineralization was measured via 10 d incubation: 10 g of air-dried soil were brought to 20% gravimetric moisture, placed in a beaker that was then placed in a 450 mL Mason jar with ~5 mL of purified water on the bottom for maintaining high humidity within the jar. Mason~~

서식 지정함: 글꼴 색: 자동

서식 있음: 들여쓰기: 첫 줄: 1.41 cm

서식 지정함: 글꼴: 기울임꼴

서식 지정함: 글꼴: 기울임꼴

서식 있음: 들여쓰기: 첫 줄: 1.41 cm

151 jars were kept in the dark at 20 °C for 10 days, and CO<sub>2</sub> concentration in the headspace was measured for each jar  
152 using Infrared Photoacoustic Spectroscopy (INNOVA Air Tech Instruments, Denmark).

### 153 **2.3 Soil core scanning and pore structure analysis**

154 Soil cores were subjected to X-ray computed micro-tomography (North Star Imaging, X3000, Rogers, USA) to  
155 visualize and quantify soil pore structure. X-ray μCT is particularly suitable for biopore investigation (Wendel et  
156 al., 2022), enabling the examination of accumulated evidence of past root-soil interactions (Helliwell et al., 2013).  
157 The scanning was conducted with a projection energy level of 75 KV and 450 μA, with 2880 projections per scan.  
158 3D reconstruction of the images was computed using efX-CT software (North Star Imaging, Rogers, USA)  
159 obtaining a final scanning resolution of 18.2 μm.

160 Reconstructed images were processed using Fiji software (Schindelin et al., 2012) and simpleITK  
161 package in Python (Beare et al., 2018). A series of image pre-processing steps was conducted using Fiji and its  
162 Xlib plugin (Münch and Holzer, 2008). Specifically, images were cropped into 1500 x 1500 pixels with a height  
163 of 2240 pixels to remove artifacts near core edges. Then, a 2D non-local filter (sigma=0.1) was applied to reduce  
164 noise.

165 For pore segmentation, threshold values were obtained from eight segmentation methods, i.e., Otsu,  
166 Kitler, Huang, Triangle, ISO, Li, Renyi, and Moments. Outliers that exceeded >1 standard deviation of the mean  
167 were removed. This approach enabled us to minimize the side effects of using one specific thresholding method  
168 and ensured robustness of the segmentation (Schlüter et al., 2014). Hereafter, we refer to the >18.2 μm Ø pores  
169 as visible pores, and their total volume as visible porosity. Pore size distributions of visible pores were determined  
170 by the Local Thickness method embedded in Fiji, which is based on maximal inscribed spheres approach (Silin  
171 and Patzek, 2006). For biopore identification, the images were subjected to Tubeness filtering in Fiji to detect  
172 tubular type pores of different radius. Detailed procedures for biopore segmentation are publicly available  
173 ([https://github.com/Maik-Lu/Roots\\_and\\_Biopores](https://github.com/Maik-Lu/Roots_and_Biopores)) (Lucas et  
174 al., 2022). Total volumes of visible pores and biopores were presented as visible porosity and bioporosity. Surface  
175 area of biopores was calculated by applying assumption that the biopore shape is cylindrical in a given radius, and  
176 the averagemean distance of soil matrix to biopores was calculated using the Euclidean Distance Transform (3D)  
177 function in Fiji. (Lucas et al., 2025).

178

### 179 **2.4 Plant diversity indicators**

180 Two plant diversity indicators were used in this study: i) plant species richness, and ii) plant functional  
181 richness (Díaz and Cabido, 2001). Plant species richness was represented by the number of plant species in each  
182 treatment, i.e., 0, 1, 2, 6, 10, and 30 for CE1, CE7, CE8, CE9, CE10, and CE12, respectively. For plant functional  
183 richness we adopted the ecological concept of plant functional types, used to simplify plant diversity and behavior  
184 in ecological models (McMahon et al., 2011). Specifically, we followed the approach used in grassland studies  
185 (Mangan et al., 2011; Spiesman et al., 2018; Tilman et al., 2006) by separating species based on different  
186 photosynthetic pathways (C3 vs. C4), and leaf shape (broad-leaf vs. grasses) to form three functional groups,

서식 있음: 둘째쓰기: 첫 줄: 1.41 cm

서식 있음: 둘째쓰기: 첫 줄: 1.41 cm

187 namely, C3 grasses, C4 grasses, and forbs. Based on species characteristics (Table S1), plant functional richness  
188 of each treatment was equal to 0, 1, 2, 2, 3, and 3 for CE1, CE7, CE8, CE9, CE10, and CE12, respectively.  
189

## 190 2.5 Statistical analysis

191 The statistical model for SOC, total soil-C, N, C:N ratio, 10-day mineralization, visible porosity, and 서식 있음: 뜯어쓰기: 첫 줄: 1.41 cm  
192 bioporosity data consisted of plant system as a fixed effect, and experimental blocks and blocks by systems  
193 interaction as random effects (Milliken and Johnson, 2009). The latter term, in essence, represents experimental  
194 plots and was used as an error term to test the plant system effect. The statistical model for the aboveground  
195 biomass measured during two consecutive years further included year and its interaction with the plant system as  
196 fixed factors. The statistical model for pore and biopore size distribution data also included the pore size class and  
197 size-by-its interaction with plant system interaction as fixed effects, and soil core nested within the plant system  
198 and experimental plot as the random effect. When the ANOVA was significant, all pairwise mean comparisons  
199 among plant systems were conducted within each pore size class. Normality was checked by visual inspection of  
200 normal probability plots, and when found violated, the data were subjected to either square root or lognormal  
201 transformation prior to the analyses. The equal variance assumption was tested by Levene's test, and when found  
202 to be violated, the unequal variance model was fitted using the approach suggested by Milliken and Johnson  
203 (2009).\_

204 To explore associations of soil characteristics with pore and biopore data, the porosity and bioporosity  
205 from two intact cores of each plot were averaged, followed by linear regression analysis. All statistical analyses  
206 were conducted using SAS 9.4 software, using PROC MIXED and PROC REG procedure. Results are reported  
207 as statistically significant at  $p < 0.05$  and as trends at  $p < 0.1$ . P-values  $< 0.1$ ,  $< 0.05$ , and  $< 0.01$  are marked with \*,  
208 \*\*, and \*\*\*, respectively.

209

## 210 3 Results

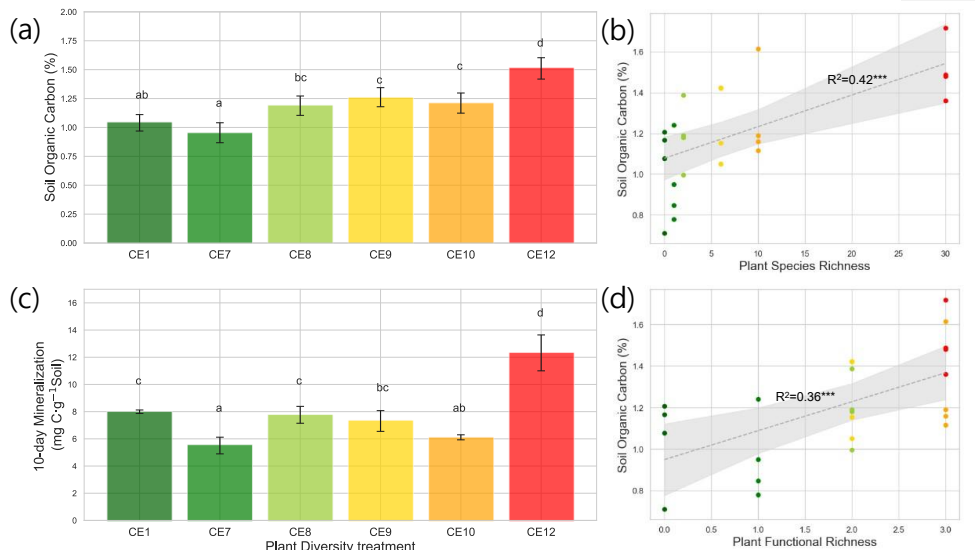
### 211 3.1 Plant biomass and soil-C characteristics of the studied plant systems

212 Total aboveground biomass (2018-2019) tended to be higher in the most diverse systems (CE10 and CE12) than  
213 in grass-only systems (CE8 and CE9), while the monoculture switchgrass (CE7) was intermediate ( $p < 0.10$ , Fig.  
214 S1b). Total aboveground biomass was weakly correlated with plant species richness (Fig. S2a) and not correlated  
215 with plant functional richness (Fig. S2b). Total aboveground biomass was not correlated with SOC contents (Fig.  
216 S2c).

217 \_The plant systems with the highest diversity (CE12) had markedly higher SOC as compared to the rest \_ of the systems (Fig. 1a). However, an increase in plant diversity from a two-species (CE8) to six-species (CE9)  
218 and then to a ten-species (CE10) system did not affect SOC (Fig. 1a). Soil C:N ratio was smallest in monoculture  
219 switchgrass (CE7), and greatest in high diversity systems (CE10 and CE12) ( $p < 0.01$ , Fig. S3). CarbonC  
220 mineralization was highest in CE12, followed by bare soil (CE1), and CE8 (Fig. 1c). C mineralization was lowest  
221 in CE7 and CE10.\_

223

224



225  
226  
227  
228  
229  
230  
231  
232  
233  
234

**Figure 1: Soil Organic Carbon (SOC) content (a) and 10-day mineralization (c) across different plant diversity systems in the studied plant diversity systems (CE1: Bare soil, CE7: Switchgrass, CE8: Switchgrass + Rye, CE9: 6 grasses, CE10: 6 grasses + 4 forbs, CE12: 6 grasses + 10 forbs). Correlations between SOC and Plant Species Richness (b), as well as Plant Functional Richness (d), are shown. Letters indicate significant differences between among plant diversity treatments ( $p < 0.05$ ). Dotted gray lines in (b) and (d) represent fitted regression models, with light gray shaded area denoting 95% confidence interval.  $R^2$  values are provided for each model. Asterisks (\*\*\*\*) indicate statistically significant regression models at  $p < 0.01$ .**

235 3.2 Biopore characteristics

236 Plant systems affected pore size distributions (Fig. 2a), where CE8, CE10, and CE12 had the lowest volumes of  
237 < 200  $\mu\text{m}$  diameter pores and the highest volumes of >400  $\mu\text{m}$  diameter pores, while an opposite trend was  
238 observed for CE1, CE7, and CE9 systems. Biopores, which was segmented based on its tubular morphology,  
239 tended to be larger than regular pores of arbitrary shapes (Fig. 2). For example, while the mode (i.e., the most  
240 frequent value) pore diameter of the entire pore size distribution was  $\sim$ 100  $\mu\text{m}$  (Fig. 2a), for biopores the modal  
241 pore diameter was  $\sim$ 300  $\mu\text{m}$  (Fig. 2b).

Visible porosity (pores of > 18.2  $\mu\text{m}$  diam.) was highest in CE9 followed by CE8 (Fig. 3a). In contrast to visible porosity, bioporosity was the highest in CE8, which is comprised of switchgrass and Canadian ryegrass (Fig. 3b). In addition to CE8, throughout the entire range of biopore sizes, CE10 and CE12 also had consistently higher biopore volumes (Fig. 2b) as well as higher total bioporosity than the rest of the systems (Fig. 3b). Total

서식 지정함: 글꼴: 9 pt

서식 지정함: 글꼴: 9 pt, 굵게

### 서식 있음: 표준

서식 지정함: 글꼴: 9 pt, 굵게

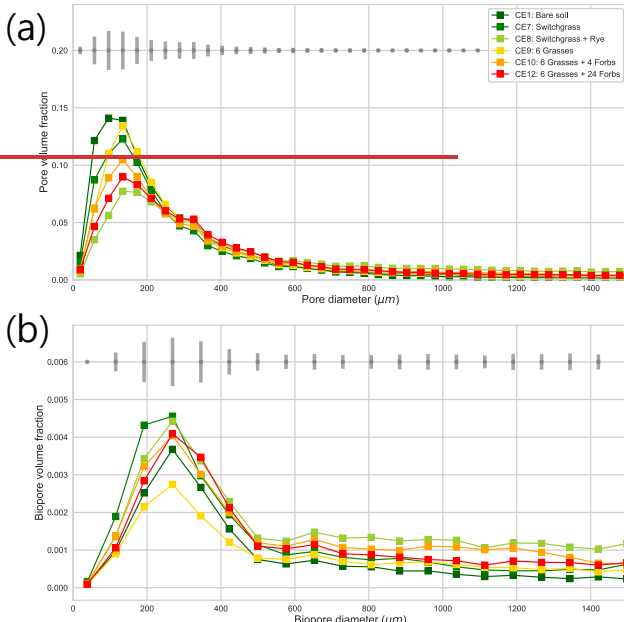
서식 지정함: 글꼴: 9 pt, 굵게

서식 지정함: 글꼴 9 pt 굵게 위 철자

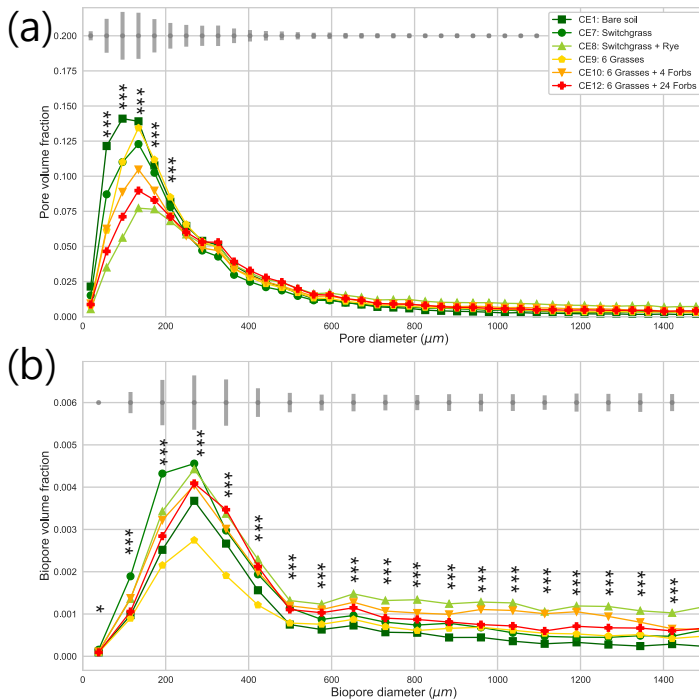
서식 지정함: 글꼴: 9 pt, 굵게

246 surface areas of biopores (all pores of < 1500  $\mu\text{m}$  diam.) were highest in CE7 and CE8, and lowest in CE1 ( $p <$   
247 0.05, Fig. 4a). AverageMean distance of soil matrix to biopores showed an opposite trend from surface area, i.e.,  
248 farthest in CE1 and CE9 and shortest in CE8 ( $p < 0.05$ , Fig. 4d).

249



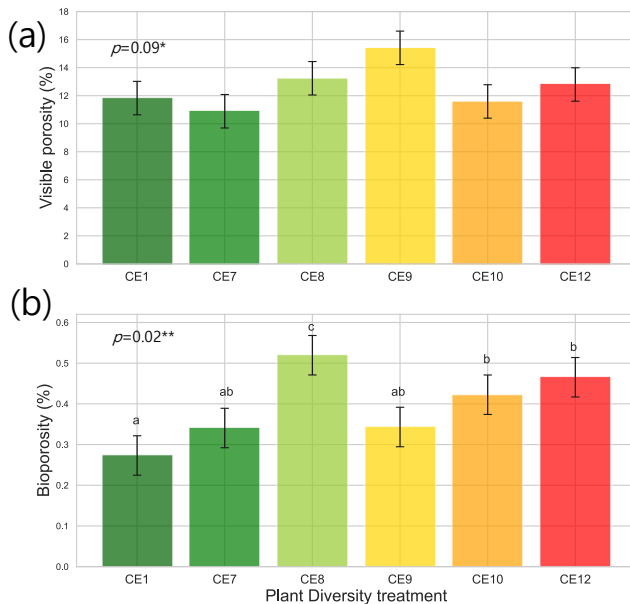
250



251

252

253 **Figure 2: Pore size distribution (a) and biopore size distribution (b) in different the studied plant diversity systems.**  
 254 **(CE1: Bare soil, CE7: Switchgrass, CE8: Switchgrass + Rye, CE9: 6 grasses, CE10: 6 grasses + 4 forbs, CE12: 6 grasses**  
 255 **+ 10 forbs). Gray bars indicate the least significant difference (LSD) in each (Bio)pore diameter group. Asterisks \*\*\***  
 256 **and \* mark significant differences among the plant diversity treatments at each (Bio)pore diameter at  $p < 0.01$  and  $p <$**   
 257 **0.10 significance.**



259  
260 **Figure 3: Visible porosity (a) and bioporosity (b) in different the studied plant diversity systems: (CE1: Bare soil, CE7:**

261 **Switchgrass, CE8: Switchgrass + Rye, CE9: 6 grasses, CE10: 6 grasses + 4 forbs, CE12: 6 grasses + 10 forbs).** Asterisks

262 \* and \*\* indicate statistically significant differences among plant diversity treatments at  $p < 0.10$  and  $0.05$ , respectively.

263 Letters indicate significant differences between among plant diversity treatments ( $p < 0.05$ ).

서식 지정함: 글꼴: 9 pt, 굵기

264 **3.3 Correlation between plant diversity, pore characteristics, and soil organic carbon (SOC)**

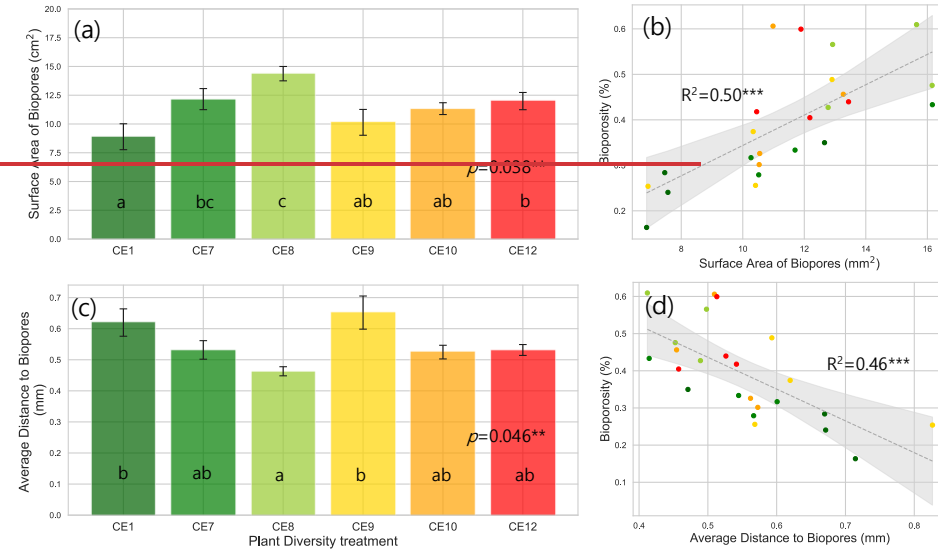
265 Overall, plant species richness and plant functional richness were both positively correlated with SOC, with plant species richness explaining 42% of the variance in SOC variation ( $p < 0.01$ ; Fig. 1b) and plant functional richness explaining 36% of SOC ( $p < 0.01$ ; Fig. 1d). The Within the pore metrics, biopore surface area of biopores was positively correlated with bioporosity with an  $R^2$  of 0.50 ( $p < 0.01$ ; Fig. 4b). On the other hand, average mean distance to biopores from the soil matrix to the nearest biopore was negatively associated with bioporosity, with an  $R^2$  of 0.46 ( $p < 0.01$ ; Fig. 4d). Visible porosity was not correlated with bioporosity increased with plant species diversity. Species richness (Fig. S4b). Bioporosity was significantly affected by plant species richness ( $p < 0.01$ ), which explained 10% of the variance in bioporosity variation ( $p < 0.01$ ; Fig. S4a). In contrast to plant species richness, plant functional richness explained 29% of the variance in bioporosity ( $p < 0.05$ ; Fig. 5a). Total visible porosity was not correlated with SOC (Fig. S4b), while Consistent with these patterns, bioporosity was positively correlated with SOC with an  $R^2$  of 0.36 ( $p < 0.01$ ; Fig. 5b).

서식 있음: 틀여쓰기: 첫 줄: 1.41 cm

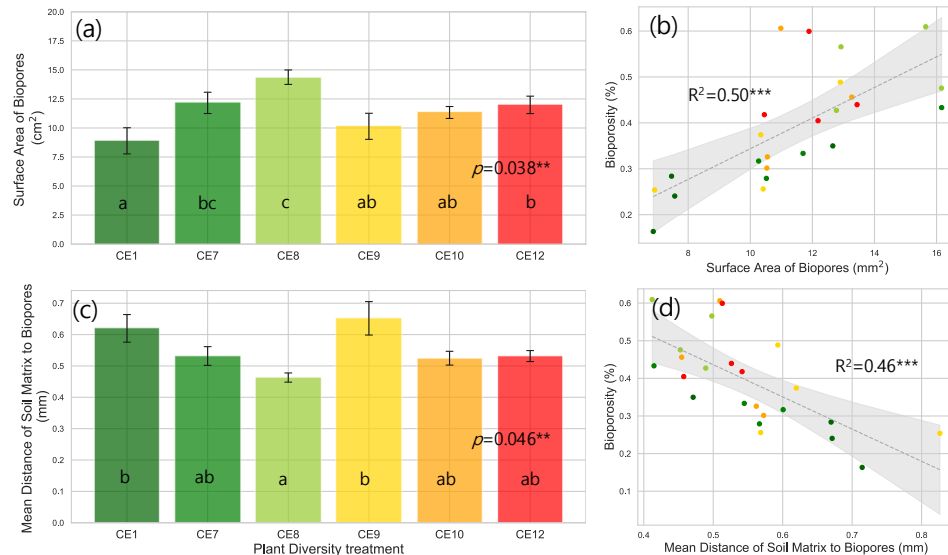
서식 지정함: 위 첨자

서식 지정함: 위 첨자

서식 지정함: 위 첨자



279

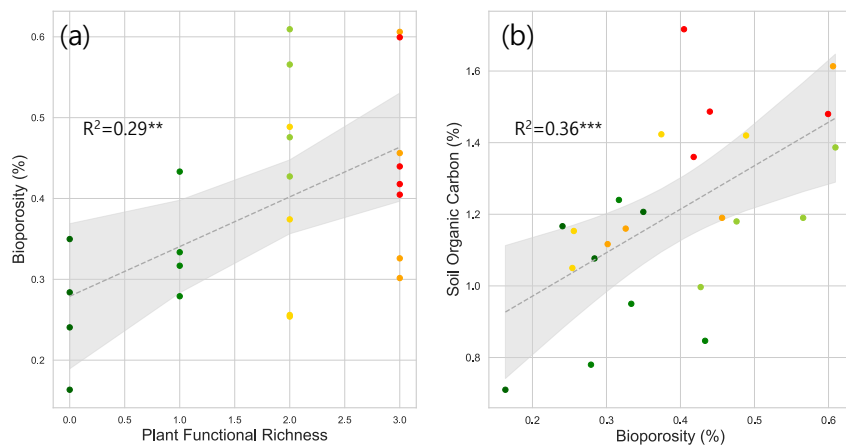


280

281 **Figure 4: Surface area of biopores (a) and average mean distance of soil matrix to biopores (c) across different in the**  
282 **studied plant diversity systems. (CE1: Bare soil, CE7: Switchgrass, CE8: Switchgrass + Rye, CE9: 6 grasses, CE10: 6**  
283 **grasses + 4 forbs, CE12: 6 grasses + 10 forbs).** Correlations between bioporosity and surface area of biopores (b), as  
284 **well as average mean distance of soil matrix to biopores (d), are shown. Letters indicate significant differences**  
285 **between among plant diversity treatments ( $p < 0.05$ ). Dotted gray lines in (b) and (d) represent fitted regression models,**

286 with light gray shaded area denoting 95% confidence interval.  $R^2$  values are provided for each model. Asterisks (\*\*\*)  
287 indicate statistically significant regression models at  $p < 0.01$ .  
288

서식 지정함: 글꼴: 10 pt, 위 첨자



290 Figure 5: Correlation between plant functional richness and bioporosity (a), and between bioporosity and soil-organic  
291 carbon SOC (b).  $R^2$  values are provided for each model. Dotted gray lines represent fitted regression  
292 models, with light gray shaded area denoting 95% confidence interval. Asterisks \*\* and \*\*\* indicate statistically significant  
293 regression models at  $p < 0.05$  and  $0.01$ , respectively.

## 294 4 Discussion

### 295 4.1 Biopores link plant diversity and SOC accumulation

296 Consistent with our expectations and previous literature (Lange et al., 2015; Prommer et al., 2020; Yang  
297 and Tilman, 2020), 12 years of contrasting plant system vegetation was sufficient to develop differences in SOC  
298 among the studied plant systems, with the highest SOC observed in the soil under the most diverse plant  
299 system community (Fig. 1a, b, and d). However, the lack of correlation between the plant aboveground biomass  
300 and SOC observed here (Fig. S2c) suggests that greater plant biomass did not itself significantly contribute to  
301 SOC increases. This lack of impact is even more obvious when comparing CE7 (monoculture) and CE8 (two-  
302 species system), where CE8 had the lowest aboveground biomass but its SOC was comparable to that from the  
303 systems with 3~5 times higher plant species richness and higher aboveground biomass (CE9 and 10, Fig. 1a and  
304 S1b).

305 Besides plant diversity, The positive association between SOC and bioporosity was another  
306 characteristic result consistent with SOC results of the study your expectations (Fig. 5b). Since the The correlation  
307 between plant richness and SOC might have been amplified due to a wide range of plant richness (specifically was  
308 largely driven by the highest species richness =of 30, which was a high leverage point in our regression analysis  
309 (Fig. 1b and d). Thus, even though the  $R^2$  for bioporosity-might-SOC regression was lower than that from  
310 species richness-SOC (0.36 vs. 0.42), bioporosity could be viewed as a better indicator predictor of SOC. Moreover,  
311 the CE8 system with its unexpectedly high SOC turned out to have higher bioporosity and higher volumes of

서식 지정함: 글꼴 색: 자동

서식 있음: 들여쓰기: 첫 줄: 1.41 cm

312 biopores of all sizes than the other studied systems (Fig. 3b), a trend that was present for all studied biopore sizes  
313 (Fig. Figs. 2b). Carbon processing in root originated biopores and 3b. This observation is more rapid than in  
314 bulk soil, since higher consistent with previous reports identifying biopores as sites of high inputs of organielable  
315 substrates (e.g., root exudates) promote growth and assimilation of C by soil microbes (Kuzyakov and  
316 Blagodatskaya, 2015) and consequently increases Pierret et al., 1999; Xiong et al., 2022), increased microbial  
317 abundance and activity (Wendel et al., 2022), and enhanced necromass accumulation (Banfield et al., 2018), all  
318 of which highlight the role of biopores in contributing to SOC accrual.

319 The biopores in CE8 had the greatest surface area of biopores, followed by the most diverse system (Fig.  
320 4a). The average mean distance of soil matrix to biopores was the shortest in CE8, followed by diverse systems  
321 (CE10 and CE12) (Fig. 4c). The surface area of biopores is critical as it represents the specific portion of the soil  
322 matrix that directly intercepts root-derived carbon inputs, i.e., rhizodeposits (Keller et al., 2021) and decomposed  
323 root residues processed by soil microbes (Kim et al., 2022). A shorter average mean distance from soil matrix to  
324 biopores indicates greater accessibility for that root-derived carbon was accessible to a large community of soil  
325 microorganisms, probably facilitating its efficient transfer and sequestration of microbially processed C into the  
326 soil matrix— (Kravchenko et al., 2019). These findings emphasize the currently underestimated importance of  
327 formation, abundance, and surface properties of biopores in affecting soil biochemical status, specifically,  
328 influencing plant-derived inputs and their potential protection within the soil matrix. Our study suggests that this  
329 role might be particularly pronounced in ecosystems with high plant species diversity.  
330 Biopores are pore spaces that have been impacted by roots and thus reflect root growth, death, and resulting  
331 changes in the soil's physicochemical properties accumulated for 12 years. In ecosystems with high plant species  
332 diversity, the importance of biopore characteristics is further amplified. Diverse plant communities exhibit  
333 complex root architectures due to interspecific interactions, leading to varying quantities and spatial distributions  
334 of root-derived carbon. Increased root originated bioporosity also indicates diversified root growth paths, which  
335 leads to strengthened root soil contact (Lucas et al., 2023). A greater interface with the soil matrix (i.e., surface  
336 area) facilitates diffusion and storage of microbially processed C (Kravchenko et al., 2019), thereby contributing  
337 to increased SOC.

338 Our C mineralization results (Fig. 1c) did not much correspond with previous reports indicating that  
339 higher plant diversity enhances microbial C use efficiency (Eisenhauer et al., 2009), likely driven by greater  
340 chemical heterogeneity and enhanced substrate accessibility to soil microbes (Mellado-Vázquez et al., 2016;  
341 Domeignoz-Horta et al., 2024). We suggest that future studies incorporate more detailed assessments of microbial  
342 biomass, community composition, and diversity to better elucidate carbon processes occurring in biopores. These  
343 inconsistencies highlight the need for further investigation of microbial activities and net C balance to identify the  
344 specific microbial pathways operating in biopores. In particular, the integration of X-ray  $\mu$ CT with pore-scale  
345 microbial analyses, as recently demonstrated by Li et al. (2024), represents a promising approach to advance our  
346 understanding of SOC accumulation mediated by soil microorganisms in biopores structures.

서식 지정함: 영어(미국)

서식 지정함: 영어(미국)

서식 지정함: 영어(미국)

서식 지정함: 영어(미국)

348 **4.2 Future research directions: winning plant species combinations?**

349 Interestingly, while bioporosity was not affected by the number of plant species within the system, it was  
350 positively correlated with the systems' functional diversity (Fig. 5a). This implies that greater diversity of  
351 functional groups – rather than a greater diversity of plant species per se – may lead to a more thorough exploration  
352 of the soil matrix in part through biopore formation, subsequently enhancing ~~soil~~-CSOC accumulation.

353 Moreover, our results suggest that certain combinations of ~~specific~~ plant species, e.g., CE8 (Switchgrass  
354 + Canadian rye~~in this study~~) can be more “effective” in building biopores, and potentially furthering SOC  
355 accumulation through rapid processing of added substrates (Banfield et al., 2017; Banfield et al., 2018). We  
356 hypothesize that Canadian rye could be viewed as a species with a keystone effect on bioporosity and SOC  
357 accumulation.

358 A “keystone effect” refers to beneficial effect of ~~specific~~a certain plant species on ecosystem function~~–~~  
359 (Mills et al., 1993). For instance, legume species added to grasslands have been found to disproportionately affect  
360 biomass productivity and root C accrual (Minns et al., 2001; Fornara and Tilman, 2008; Lange et al., 2015; Yang  
361 et al., 2019) due to N assimilation by legumes and consequent utilization of that N by grasses (Minns et al., 2001;  
362 Mangan et al., 2011; Mou et al., 2024). Introduction of a C3 plant, i.e., Canadian rye, into a monoculture C4  
363 switchgrass community may have altered switchgrass root growth and exudation patterns. ~~Sensitivity~~This  
364 conjecture is supported by a report on sensitivity of chemical composition of switchgrass root exudates to  
365 ~~neighboring~~neighbouring plant species (e.g., C3 *Koeleria macrantha* Ledeb.), and resultant with subsequent  
366 increases in microbial biomass C and changes in bacterial diversity in the switchgrass rhizosphere ~~have indeed~~  
367 ~~been demonstrated before~~–(Ulbrich et al., 2022). We see the need for further investigation into the role that  
368 individual members of grassland communities may play in stimulating soil pore structure development and ~~soil~~  
369 ~~ESOC~~ accumulation. Identifying keystone species enabling more efficient C accumulation can guide plant  
370 restoration and SOC accrual efforts.–

371 **5. Conclusion**

372 The 12-year grassland experiment demonstrates that SOC accumulation is governed by plant diversity, with the  
373 benefits of high plant diversity being, in part, exhibited via development of biopores. Yet, certain species  
374 combinations may lead to biopore formation and SOC accumulation benefits disproportional to the actual level  
375 of the plant system diversity. Specifically, the two-species mixture of C4 switchgrass and C3 Canadian rye created  
376 the greatest bioporosity, shortest mean soil-to-pore distance, and the largest biopore surface area, thereby  
377 accelerating microbial processing and stabilization of root-derived C in the surrounding matrix. These findings  
378 highlight bioporosity as a more reliable proxy for SOC gains than plant species number alone, and point to  
379 potential existence of specific “keystone” species combinations that may disproportionately enhance soil structure  
380 and C sequestration. Identifying and deploying such functionally complementary plant species can offer a targeted  
381 pathway for optimizing grassland restoration and long-term SOC storage.

서식 있음: 들여쓰기: 첫 줄: 1.41 cm

서식 지정함: 글꼴: 기울임꼴

382 **Acknowledgements**

서식 지정함: 글꼴 색 자동

383 This work was supported by a 2019 Kellogg Biological Station LTER Fellowship. Support for this research was  
384 provided by the U.S. Department of Energy, Office of Science, Office of Biological and Environmental Research  
385 (Award DE-SC0018409), by the National Science Foundation Long-term Ecological Research Program (DEB  
386 2224712) at the Kellogg Biological Station, and by Michigan State University AgBioResearch. This work was  
387 also supported by the New Faculty Startup Fund from Seoul National University.

388

389 **Code/Data availability**

서식 지정함: 글꼴 색 자동

390 The datasets generated during and/or analyzed during the current study are available upon request.

391 **Author contribution**

서식 지정함: 글꼴 색 자동

392 K. K Formal analysis, investigation, Writing-original draft, visualization  
393 M.G: Software, Validation, Writing-Review & Editing  
394 G. P. R: Resources, Project administration, Writing-Review & Editing  
395 A. K: Conceptualization, Resources, Writing-Review & Editing, Supervision, Funding acquisition

396 **Competing interests**

서식 지정함: 글꼴 색 자동

397 The authors declare that they have no known competing financial interests or personal relationships that could  
398 have appeared to influence the work reported in this paper.

399 **References**

서식 지정함: 글꼴 색 자동

400 Banfield, C.C., Dippold, M.A., Pausch, J., Hoang, D.T., Kuzyakov, Y., 2017. Biopore history determines the  
401 microbial community composition in subsoil hotspots. *Biology and Fertility of Soils* 53, 573-588.  
402 Banfield, C.C., Pausch, J., Kuzyakov, Y., Dippold, M.A., 2018. Microbial processing of plant residues in the  
403 subsoil—The role of biopores. *Soil Biology and Biochemistry* 125, 309-318.  
404 Bargaz, A., Noyce, G.L., Fulthorpe, R., Carlsson, G., Furze, J.R., Jensen, E.S., Dhiba, D., Isaac, M.E., 2017.  
405 Species interactions enhance root allocation, microbial diversity and P acquisition in intercropped wheat and  
406 soybean under P deficiency. *Applied Soil Ecology* 120, 179-188.  
407 Beare, R., Lowekamp, B., Yaniv, Z., 2018. Image segmentation, registration and characterization in R with  
408 SimpleITK. *Journal of statistical software* 86.  
409 Berhongaray, G., Cotrufo, F.M., Janssens, I.A., Ceulemans, R., 2019. Below-ground carbon inputs contribute  
410 more than above-ground inputs to soil carbon accrual in a bioenergy poplar plantation. *Plant and soil* 434, 363-  
411 378.  
412 Blackwell, P., Green, T., Mason, W., 1990. Responses of biopore channels from roots to compression by vertical  
413 stresses. *Soil Science Society of America Journal* 54, 1088-1091.  
414 Bolte, A., Villanueva, I., 2006. Interspecific competition impacts on the morphology and distribution of fine roots  
415 in European beech (*Fagus sylvatica* L.) and Norway spruce (*Picea abies* (L.) Karst.). *European Journal of Forest  
416 Research* 125, 15-26.  
417 Chen, H., Mommer, L., Van Ruijven, J., De Kroon, H., Fischer, C., Gessler, A., Hildebrandt, A., Scherer-Lorenzen,  
418 M., Wirth, C., Weigelt, A., 2017. Plant species richness negatively affects root decomposition in grasslands.  
419 *Journal of Ecology* 105, 209-218.

420 Cotrufo, M.F., Haddix, M.L., Kroeger, M.E., Stewart, C.E., 2022. The role of plant input physical-chemical  
421 properties, and microbial and soil chemical diversity on the formation of particulate and mineral-associated  
422 organic matter. *Soil Biology and Biochemistry* 168, 108648.

423 Dexter, A., 1986. Model experiments on the behaviour of roots at the interface between a tilled seed-bed and a  
424 compacted sub-soil: III. Entry of pea and wheat roots into cylindrical biopores. *Plant and soil* 95, 149-161.

425 Diaz, S., Cabido, M., 2001. Vive la différence: plant functional diversity matters to ecosystem processes. *Trends  
426 in ecology & evolution* 16, 646-655.

427 Domeignoz-Horta, L.A., Cappelli, S.L., Shrestha, R., Gerin, S., Lohila, A.K., Heinonsalo, J., Nelson, D.B.,  
428 Kahmen, A., Duan, P., Sebag, D., 2024. *Plant diversity drives positive microbial associations in the rhizosphere  
429 enhancing carbon use efficiency in agricultural soils. Nature communications* 15, 8065.

430 Eisenhauer, N., Lanoue, A., Strecker, T., Scheu, S., Steinauer, K., Thakur, M. P., & Mommert, L., 2017. *Root  
431 biomass and exudates link plant diversity with soil bacterial and fungal biomass. Scientific reports*, 7(1), 1-8.

432 Fornara, D., Tilman, D., 2008. Plant functional composition influences rates of soil carbon and nitrogen  
433 accumulation. *Journal of Ecology* 96, 314-322.

434 Eisenhauer, N., Milcu, A., Sabais, A.C., Bessler, H., Weigelt, A., Engels, C., Scheu, S., 2009. *Plant community  
435 impacts on the structure of earthworm communities depend on season and change with time. Soil Biology and  
436 Biochemistry* 41, 2430-2443.

437 Gersani, M., Brown, J.S., O'Brien, E.E., Maina, G.M., Abramsky, Z., 2001. *Tragedy of the commons as a result  
438 of root competition. Journal of Ecology* 89, 660-669.

439 Guhra, T., Stolze, K., Totsche, K.U., 2022. *Pathways of biogenically excreted organic matter into soil aggregates. Soil  
440 Biology and Biochemistry* 164, 108483.

441 Halli, H. M., Govindasamy, P., Choudhary, M., Srinivasan, R., Prasad, M., Wasnik, V. K., Yadav, V., Singh,  
442 A.K., Kumar, S., Vijay, D., and Pathak, H. (2022). *Range grasses to improve soil properties, carbon sustainability,  
443 and fodder security in degraded lands of semi-arid regions. Science of the Total Environment*, 851, 158211.

444 Helliwell, J.R., Sturrock, C.J., Grayling, K.M., Tracy, S.R., Flavel, R., Young, I., Whalley, W., Mooney, S.J.,  
445 2013. Applications of X-ray computed tomography for examining biophysical interactions and structural  
446 development in soil systems: a review. *European Journal of Soil Science* 64, 279-297.

447 Hoang, D.T., Pausch, J., Razavi, B.S., Kuzyakova, I., Banfield, C.C., Kuzyakov, Y., 2016. *Hotspots of microbial  
448 activity induced by earthworm burrows, old root channels, and their combination in subsoil. Biology and Fertility  
449 of Soils* 52, 1105-1119.

450 Kautz, T., 2015. Research on subsoil biopores and their functions in organically managed soils: A review.  
451 *Renewable Agriculture and Food Systems* 30, 318-327.

452 Keller, A.B., Brzostek, E.R., Craig, M.E., Fisher, J.B., Phillips, R.P., 2021. Root-derived inputs are major  
453 contributors to soil carbon in temperate forests, but vary by mycorrhizal type. *Ecology letters* 24, 626-635.

454 Kim, K., Gil, J., Ostrom, N.E., Gandhi, H., Oerther, M.S., Kuzyakov, Y., Guber, A.K., Kravchenko, A.N., 2022.  
455 Soil pore architecture and rhizosphere legacy define N2O production in root detritusphere. *Soil Biology and  
456 Biochemistry* 166, 108565.

457 Kravchenko, A., Guber, A., Razavi, B., Koestel, J., Quigley, M., Robertson, G., Kuzyakov, Y., 2019. Microbial  
458 spatial footprint as a driver of soil carbon stabilization, *Nat. Commun.*, 10, 3121.

459 Kravchenko, A.N., Zheng, H., Kuzyakov, Y., Robertson, G.P., Guber, A.K., 2021. *Belowground interplant carbon  
460 transfer promotes soil carbon gains in diverse plant communities. Soil Biology & Biochemistry* 159.

461 Kuzyakov, Y., Blagodatskaya, E., 2015. Microbial hotspots and hot moments in soil: concept & review. *Soil  
462 Biology and Biochemistry* 83, 184-199.

463 Kuzyakov, Y., Kooch, Y., 2024. *Earthworm Biopores for Transport and Nutrient Cycling. Earthworms and  
464 Ecological Processes. Springer*, pp. 417-432.

465 Lange, M., Eisenhauer, N., Sierra, C.A., Bessler, H., Engels, C., Griffiths, R.I., Mellado-Vázquez, P.G., Malik,  
466 A.A., Roy, J., Scheu, S., 2015. Plant diversity increases soil microbial activity and soil carbon storage. *Nature  
467 communications* 6, 6707.

468 Larnaudie, V., Ferrari, M.D., Lareo, C., 2022. Switchgrass as an alternative biomass for ethanol production in a  
469 biorefinery: Perspectives on technology, economics and environmental sustainability. *Renewable and Sustainable  
470 Energy Reviews* 158, 112115.

471 Lee, J.H., Lucas, M., Guber, A.K., Li, X., Kravchenko, A.N., 2023. Interactions among soil texture, pore structure,  
472 and labile carbon influence soil carbon gains. *Geoderma* 439, 116675.

473 Lee, J.H., Ulbrich, T.C., Oerther, M., Kuzyakov, Y., Guber, A.K., Kravchenko, A.N., 2025. *Belowground plant  
474 carbon and nitrogen exchange: plant-derived carbon inputs and pore structure formation. Soil Biology and  
475 Biochemistry* 207, 109833.

476 Li, Z., Kravchenko, A.N., Cupples, A., Guber, A.K., Kuzyakov, Y., Philip Robertson, G., Blagodatskaya, E., 2024.  
477 *Composition and metabolism of microbial communities in soil pores. Nature communications* 15, 3578.

서식 지정함: 글꼴: 10 pt

478 Lehmann, J., Hansel, C.M., Kaiser, C., Kleber, M., Maher, K., Manzoni, S., Nunan, N., Reichstein, M., Schimel,  
 479 J.P., Torn, M.S., 2020. Persistence of soil organic carbon caused by functional complexity. *Nature Geoscience* 13,  
 480 529-534.

481 Liebman, M., Helmers, M.J., Schulte, L.A., Chase, C.A., 2013. Using biodiversity to link agricultural productivity  
 482 with environmental quality: Results from three field experiments in Iowa. *Renewable Agriculture and Food  
 483 Systems* 28, 115-128.

484 Lucas, M., Nguyen, L.T., Guber, A., Kravchenko, A.N., 2022. Cover crop influence on pore size distribution and  
 485 biopore dynamics: Enumerating root and soil faunal effects. *Frontiers in Plant Science* 13, 928569.

486 Lucas, M., Santiago, J.P., Chen, J., Guber, A., Kravchenko, A., 2023. The soil pore structure encountered by roots  
 487 affects plant-derived carbon inputs and fate. *New Phytologist* 240, 515-528.

488 Mangan, M.E., Sheaffer, C., Wyse, D.L., Ehlke, N.J., Reich, P.B., 2011. Native perennial grassland species for  
 489 bioenergy: establishment and biomass productivity. *Agronomy Journal* 103, 509-519.

490 Lucas, M., Gil, J., Robertson, G., Ostrom, N., Kravchenko, A., 2025. Changes in soil pore structure generated by  
 491 the root systems of maize, sorghum and switchgrass affect in situ N<sub>2</sub>O emissions and bacterial denitrification.  
 492 *Biology and Fertility of Soils* 61, 367-383.

493 Marshall, A.H., Collins, R.P., Humphreys, M.W., Scullion, J., 2016. A new emphasis on root traits for perennial  
 494 grass and legume varieties with environmental and ecological benefits. *Food and energy security* 5, 26-39.

495 McDaniel, M.D., Tiemann, L.K., Grandy, A.S., 2014. Does agricultural crop diversity enhance soil microbial  
 496 biomass and organic matter dynamics? A meta-analysis. *Ecological Applications* 24, 560-570.

497 McMahon, S.M., Harrison, S.P., Armbruster, W.S., Bartlein, P.J., Beale, C.M., Edwards, M.E., Kattge, J.,  
 498 Midgley, G., Morin, X., Prentice, I.C., 2011. Improving assessment and modelling of climate change impacts on  
 499 global terrestrial biodiversity. *Trends in ecology & evolution* 26, 249-259.

500 Mellado-Vázquez, P.G., Lange, M., Bachmann, D., Gockele, A., Karlowsky, S., Milcu, A., Piel, C., Roscher, C.,  
 501 Roy, J., Gleixner, G., 2016. Plant diversity generates enhanced soil microbial access to recently photosynthesized  
 502 carbon in the rhizosphere. *Soil Biology and Biochemistry* 94, 122-132.

503 Milcu, A., Partsch, S., Scherber, C., Weisser, W. W., & Scheu, S., 2008. Earthworms and legumes control litter  
 504 decomposition in a plant diversity gradient. *Ecology*, 89(7), 1872-1882.

505 Milliken, G.A., Johnson, D.E., 2009. Analysis of Messy Data Volume 1. (No Title).

506 Mills, L.S., Soulé, M.E., Doak, D.F., 1993. The keystone-species concept in ecology and conservation. *BioScience*  
 507 43, 219-224.

508 Minns, A., Finn, J., Hector, A., Caldeira, M., Joshi, J., Palmborg, C., Schmid, B., Scherer-Lorenzen, M., Spehn,  
 509 E., Troumbis, A., project, t.B., 2001. The functioning of European grassland ecosystems: potential benefits of  
 510 biodiversity to agriculture. *Outlook on AGRICULTURE* 30, 179-185.

511 Mou, X., Lv, P., Jia, B., Mao, H., Zhao, X., 2024. Plant species richness and legume presence increase microbial  
 512 necromass carbon accumulation. *Agriculture, Ecosystems & Environment* 374, 109196.

513 Mueller, C.W., Baumert, V., Carminati, A., Germon, A., Holz, M., Kögel-Knabner, I., Peth, S., Schlüter, S., Uteau,  
 514 D., Vetterlein, D., 2024. From rhizosphere to detritusphere—Soil structure formation driven by plant roots and the  
 515 interactions with soil biota. *Soil Biology and Biochemistry* 193, 109396.

516 Münch, B., Holzer, L., 2008. Contradicting geometrical concepts in pore size analysis attained with electron  
 517 microscopy and mercury intrusion. *Journal of the American Ceramic Society* 91, 4059-4067.

518 Newman, E.I., Ritz, K., 1986. Evidence of the pathways of phosphorus transfer between vesicular-arbuscular  
 519 mycorrhizal plants. *New Phytologist* 104, 77-87.

520 Pierret, A., Moran, C., Pankhurst, C., 1999. Differentiation of soil properties related to the spatial association of  
 521 wheat roots and soil macropores. *Plant and soil* 211, 51-58.

522 Prommer, J., Walker, T.W., Wanek, W., Braun, J., Zezula, D., Hu, Y., Hofhansl, F., Richter, A., 2020. Increased  
 523 microbial growth, biomass, and turnover drive soil organic carbon accumulation at higher plant diversity. *Global  
 524 Change Biology* 26, 669-681.

525 Qian, Z., Li, Y., Du, H., Wang, K., Li, D., 2023. Increasing plant species diversity enhances microbial necromass  
 526 carbon content but does not alter its contribution to soil organic carbon pool in a subtropical forest. *Soil Biology  
 527 and Biochemistry* 187, 109183.

528 Quigley, M., Kravchenko, A., 2022. Inputs of root-derived carbon into soil and its losses are associated with pore-  
 529 size distributions. *Geoderma* 410, 115667.

530 Robertson, G.P., Hamilton, S.K., 2015. Long-term ecological research at the Kellogg Biological Station LTER  
 531 site. The ecology of agricultural landscapes: Long-term research on the path to sustainability 1, 32.

532 Roosendaal, D., Stewart, C.E., Denef, K., Follett, R.F., Pruessner, E., Comas, L.H., Varvel, G.E., Saathoff, A.,  
 533 Palmer, N., Sarath, G., 2016. Switchgrass ecotypes alter microbial contribution to deep-soil C. *Soil* 2, 185-197.

534 Schindelin, J., Arganda-Carreras, I., Frise, E., Kaynig, V., Longair, M., Pietzsch, T., Preibisch, S., Rueden, C.,  
 535 Saalfeld, S., Schmid, B., 2012. Fiji: an open-source platform for biological-image analysis. *Nature methods* 9,  
 536 676-682.

서식 지정함: 글꼴: 10 pt

537 Schlüter, S., Sheppard, A., Brown, K., Wildenschild, D., 2014. Image processing of multiphase images obtained  
538 via X-ray microtomography: A review. *Water Resources Research* 50, 3615-3639.

539 Silin, D., Patzek, T., 2006. Pore space morphology analysis using maximal inscribed spheres. *Physica A: Statistical mechanics and its applications* 371, 336-360.

540 Spiesman, B.J., Kummel, H., Jackson, R.D., 2018. Carbon storage potential increases with increasing ratio of C 4 to C 3 grass cover and soil productivity in restored tallgrass prairies. *Oecologia* 186, 565-576.

541 Sprunger, C.D., Robertson, G.P., 2018. Early accumulation of active fraction soil carbon in newly established  
542 cellulosic biofuel systems. *Geoderma* 318, 42-51.

543 [Tilman, D., Reich, P. B., & Knops, J. M. 2006. Biodiversity and ecosystem stability in a decade-long grassland experiment. \*Nature\*, 441\(7093\), 629-632.](#)

544 [Ulbrich, T.C., Rivas-Ubach, A., Tiemann, L.K., Friesen, M.L., Evans, S.E., 2022. Plant root exudates and rhizosphere bacterial communities shift with neighbor context. \*Soil Biology and Biochemistry\* 172, 108753.](#)

545 Wahlström, E.M., Kristensen, H.L., Thomsen, I.K., Labouriau, R., Pulido-Moncadá, M., Nielsen, J.A., Munkholm, L.J., 2021. Subsoil compaction effect on spatio-temporal root growth, reuse of biopores and crop yield of spring barley. *European Journal of Agronomy* 123, 126225.

546 Wang, B., Zhang, W., Ahanbiece, P., Gan, Y., Xu, W., Li, L., Christie, P., Li, L., 2014. Interspecific interactions alter root length density, root diameter and specific root length in jujube/wheat agroforestry systems. *Agroforestry systems* 88, 835-850.

547 Wang, X.-Y., Ge, Y., Wang, J., 2017. Positive effects of plant diversity on soil microbial biomass and activity are associated with more root biomass production. *Journal of Plant Interactions* 12, 533-541.

548 Wendel, A.S., Bauke, S.L., Amelung, W., Knief, C., 2022. Root-rhizosphere-soil interactions in biopores. *Plant and soil* 475, 253-277.

549 White, R.G., Kirkegaard, J.A., 2010. The distribution and abundance of wheat roots in a dense, structured subsoil—implications for water uptake. *Plant, cell & environment* 33, 133-148.

550 [Xiong, P., Zhang, Z., Peng, X., 2022. Root and root-derived biopore interactions in soils: A review. \*Journal of Plant Nutrition and Soil Science\* 185, 643-655.](#)

551 Yang, Y., Tilman, D., 2020. Soil and root carbon storage is key to climate benefits of bioenergy crops. *Biofuel Research Journal* 7, 1143-1148.

552 Yang, Y., Tilman, D., Furey, G., Lehman, C., 2019. Soil carbon sequestration accelerated by restoration of grassland biodiversity. *Nature communications* 10, 718.

553 [Zahorec, A., Reid, M.L., Tiemann, L.K., Landis, D.A., 2022. Perennial grass bioenergy cropping systems: Impacts on soil fauna and implications for soil carbon accrual. \*GCB Bioenergy\* 14, 4-23.](#)

554 Zegada-Lizarazu, W., Zanetti, F., Di Virgilio, N., Monti, A., 2022. Is switchgrass good for carbon savings? Long-term results in marginal land. *GCB Bioenergy* 14, 814-823.

서식 지정함: 글꼴: 10 pt

서식 지정함: 글꼴: 10 pt

서식 지정함: 글꼴: 10 pt